Astron. Astrophys. 286, 269–274 (1994)

ASTRONOMY AND ASTROPHYSICS

New contribution functions for Zeeman split spectral lines

S.K. Solanki and J.H.M.J. Bruls*

Institut für Astronomie, ETH-Zentrum, CH-8092 Zürich, Switzerland

Received 30 August 1993 / Accepted 24 December 1993

Abstract. The recently introduced emergent line radiation contribution function (Achmad et al. 1991; Gurtovenko et al. 1991) is extended to the Stokes vector of Zeeman split spectral lines. This contribution function is compared to the line depresssion contribution function on the basis of an analytical relation and of numerical NLTE computations of a set of spectral lines. In general the two contribution functions give very similar results, although in some cases the one or the other of them is more suitable.

Key words: line: formation – line: profile – polarization – Sun: magnetic fields

1. Introduction

The search for a functional description of the contribution from each atmospheric layer to a spectral line, which is not distorted by the unrelated contribution to the continuum, goes back to de Jager (1952), Pecker (1952), Mein (1971) and Gurtovenko et al. (1974). The search appeared to have ended with the consistent derivation by Magain (1986) of a unique contribution function (CF) for the intensity line depression, $R_I = 1 - I_l/I_c$, where I_l is the intensity in the line and I_c is the neighboring continuum intensity. Magain's CF, denoted by C_R, was generalized to the Stokes vector of a Zeeman split line by Grossmann-Doerth et al. (1988). Recently, however, C_R has been criticized by Achmad et al. (1991), who introduced two new CFs, one each for the emergent continuum, C_c, and for the emergent line radiation, C_l (cf. Gurtovenko et al. 1991). According to Achmad et al. these new CFs have the advantage that, unlike C_R, they can be uniquely extended to the flux spectrum. In addition, these authors found that C_R and C_l differ somewhat even for the intensity. Achmad et al. therefore recommended that their new CFs, in particular C_l, are to be preferred in all cases.

In the present paper we first extend the definition of C_l and C_R to the full Stokes vector of Zeeman split lines (Sects. 3 and 4). Then, in Sects. 5 and 6 we discuss the relative advantages and disadvantages of C_R and C_l (for Zeeman split and unsplit lines). Finally, in Sect. 7 we summarize the results.

Send offprint requests to: S.K. Solanki

* *Present address:* Big Bear Solar Observatory, Big Bear City, CA 92314, USA

2. The Achmad et al. contribution functions

In order to distinguish between the spectral line and the continuum Achmad et al. (1991) separate the total source function, S_t, into a part due to the line, S_l, and another due to the continuum, S_c.

$$S_t = \frac{\kappa_l}{\kappa_t} S_l + \frac{\kappa_c}{\kappa_t} S_c, \tag{1}$$

where κ_l is the line absorption coefficient at the wavelength under consideration, κ_c is the corresponding continuum absorption coefficient and $\kappa_t = \kappa_c + \kappa_l$. By showing that the formal solution integral for the intensity can thereby also be separated into a continuum and a line part, they obtain the following expressions for the CFs to the emergent line and continuum radiation:

$$C_l(\log \tau_0) = \ln(10)\, \tau_0 \frac{\kappa_l}{\kappa_0} S_l(\tau_t) e^{-\tau_t}, \tag{2}$$

$$C_c(\log \tau_0) = \ln(10)\, \tau_0 \frac{\kappa_c}{\kappa_0} S_c(\tau_t) e^{-\tau_t}, \tag{3}$$

where τ_0 and κ_0 are the optical depth and absorption coefficient at a reference wavelength λ_0.

3. Line and continuum CFs for the Stokes parameters

Expressions corresponding to Eqs. 2 and 3 can be derived by simple analogy for the CFs to the emergent Stokes parameters. This is best illustrated by first rewriting the transfer equation for the intensity, I, in the absence of magnetic field into the form in which the Unno-Rachkovsky equations are usually written,

$$\frac{dI}{d\tau_c} = (1 + \eta_I) I - (\eta_I S_l + S_c), \tag{4}$$

where we have made use of the fact that Eq. (1) is equivalent to

$$S_t = \frac{\eta_I}{1 + \eta_I} S_l + \frac{1}{1 + \eta_I} S_c, \tag{5}$$

with $\eta_I = \kappa_l/\kappa_c$. The formal solution for a semi-infinite atmosphere then reads:

$$I(0) = \int_0^\infty (\eta_I S_l + S_c) e^{-(1+\eta_I)\tau_c} d\tau_c$$

$$= \int_0^\infty S_c e^{-(1+\eta_I)\tau_c} d\tau_c + \int_0^\infty \eta_I S_l e^{-(1+\eta_I)\tau_c} d\tau_c. \quad (6)$$

From Eq. (6) we immediately obtain

$$C_c(\log\tau_c) = \ln(10)\,\tau_c S_c(\tau_c) e^{-(1+\eta_I)\tau_c}, \quad (7)$$

$$C_l(\log\tau_c) = \ln(10)\,\tau_c \eta_I S_l(\tau_c) e^{-(1+\eta_I)\tau_c}. \quad (8)$$

In LTE $S_c = S_l = S_t = B_\nu$ and

$$C_l = \eta_I C_c = \frac{\eta_I}{1+\eta_I} C_t, \quad (9)$$

where $C_t = C_c + C_l$ is the CF of the total emergent radiation. For large η_I (in the cores of strong lines) $C_l \approx C_t$ and $C_c \approx 0$, while $C_c \approx C_t$ and $C_l \approx 0$ for small η_I. Furthermore, in a Milne-Eddington model atmosphere (η_I independent of τ_c) $C_l \sim C_c \sim C_t$. In particular, C_l has its maximum at the same τ as C_c and C_t.

We now turn to the Stokes parameters. The Unno-Rachkovsky equations read

$$\frac{d\mathbf{I}}{d\tau_c} = (\mathbf{E}+\Omega)\mathbf{I} - (\mathbf{1}S_c + \Omega\mathbf{1}S_l), \quad (10)$$

where $\mathbf{I} = (I,Q,U,V)^T$ is the Stokes vector, $\mathbf{E}$ is the unity matrix, $\mathbf{1} = (1,0,0,0)^T$ and Ω is the absorption matrix (e.g. Landi Degl'Innocenti 1976, Rees 1987). Following Landi Degl'Innocenti (1987) we can write the formal solution as:

$$\mathbf{I}(0) = \int_0^\infty \mathbf{O}(0,\tau_c)(\Omega\mathbf{1}S_l + \mathbf{1}S_c) d\tau_c, \quad (11)$$

where $\mathbf{O}(\tau_2,\tau_1)$ is the evolution operator, defined by its differential equation

$$\frac{d\mathbf{O}(\tau_2,\tau_1)}{d\tau_2} = (\mathbf{E}+\Omega)\mathbf{O}(\tau_2,\tau_1), \quad (12)$$

with $\mathbf{O}(\tau,\tau) = \mathbf{E}$. Equation (11) is completely analogous to Eq. (6), so that we can write

$$\mathbf{C}_l(\log\tau_c) = \ln(10)\,\tau_c\,\mathbf{O}(0,\tau_c)\Omega(\tau_c)\mathbf{1}S_l(\tau_c), \quad (13)$$

$$\mathbf{C}_c(\log\tau_c) = \ln(10)\,\tau_c\,\mathbf{O}(0,\tau_c)\mathbf{1}S_c(\tau_c). \quad (14)$$

$\mathbf{C} = (C_I, C_Q, C_U, C_V)^T$ is the Stokes contribution vector.

Note that for a magnetized atmosphere the polarized components of $\mathbf{C}_c$ are non-zero, although Stokes Q, U and V show no continuum signal. Recall that the same problem is encountered when considering the contribution function to the total emission (e.g. van Ballegooijen 1985; Grossmann-Doerth et al. 1988). To understand this behavior we must recall that at a wavelength with significant line absorption $\mathbf{C}_c$ is not the continuum CF. Rather, it is the CF for the case that, in addition to continuum absorption and emission, line absorption is present (but no line emission). For a Zeeman split line such pure line absorption may be different in orthogonal polarizations at a certain wavelength, so that it can also produce polarized profiles. Only at wavelengths at which $\eta_I \approx \eta_Q \approx \eta_U \approx \eta_V \approx 0$ does $\mathbf{C}_c$ become the contribution function of the continuum.

$\mathbf{C}_l$, on the other hand, does tend to zero far from line center, since Ω approaches $\mathbf{0}$ there. Consequently, $\mathbf{C}_l$ is the useful quantity and $\mathbf{C}_c$ should in general be ignored.

4. Computing the Stokes contribution functions with the DELO technique

Next we write the expressions for $\mathbf{C}_l$ and $\mathbf{C}_c$ in the notation of the Diagonal Element Lambda Operator (DELO) technique for the solution of Eq. (10) (Rees et al. 1989). This technique has established itself as fast and stable and is widely used. In the DELO technique for the solution of the Unno-Rachkovsky equations the Stokes vector $\mathbf{I}_n$ at grid point n is related to $\mathbf{I}_{n+1}$, the Stokes vector at the deeper neighboring point $n+1$, by

$$\mathbf{I}_n = \mathbf{Q}_n\mathbf{I}_{n+1} + \mathbf{P}_n, \quad (15)$$

where

$$\mathbf{P}_n = \frac{\mathbf{R}_n}{\eta_I}\left[F_n\mathbf{S}_{t,n} + G_n(\mathbf{S}_{t,n+1} - \mathbf{S}_{t,n})\right], \quad (16)$$

$$\mathbf{Q}_n = \mathbf{R}_n\left[E_n\mathbf{E} - G_n\left(\frac{\mathbf{E}+\Omega_{n+1}}{\eta_{I,n+1}} - \mathbf{E}\right)\right]. \quad (17)$$

In Eqs. (16) and (17)

$$\mathbf{R}_n = \left[\mathbf{E} + (F_n - G_n)\left(\frac{\mathbf{E}+\Omega_n}{\eta_{I,n}} - \mathbf{E}\right)\right]^{-1} \quad (18)$$

and

$$E_n = e^{-\delta_n}, \quad (19)$$

$$F_n = 1 - e^{-\delta_n}, \quad (20)$$

$$G_n = [(1-e^{-\delta_n}) - \delta_n e^{-\delta_n}]/\delta_n, \quad (21)$$

$$\delta_n = \tau_{\nu,n+1} - \tau_{\nu,n}. \quad (22)$$

It can be easily shown that $\mathbf{Q}_n$ is the numerical equivalent of $\mathbf{O}(\tau_n,\tau_{n+1})$ and that

$$\mathbf{O}(0,\tau_n) \Longleftrightarrow \prod_{k=1}^{n-1}\mathbf{Q}_k. \quad (23)$$

Consequently

$$\mathbf{C}_c(\log\tau_n) = \ln(10)\,\tau_n \prod_{k=1}^{n-1}\mathbf{Q}_k\mathbf{1}S_c(\tau_n), \quad (24)$$

$$\mathbf{C}_l(\log\tau_n) = \ln(10)\,\tau_n \prod_{k=1}^{n-1}\mathbf{Q}_k\Omega_n\mathbf{1}S_l(\tau_n) \quad (25)$$

The computation of $\mathbf{C}_l$ and $\mathbf{C}_c$ for other techniques of the solution of the Unno-Rachkovsky equations (van Ballegooijen 1985; Rees et al. 1989) is equally straightforward.

5. Analytical relationship between $\mathbf{C}_l$ and $\mathbf{C}_R$

In this section we briefly discuss, on an analytical basis, the relationship between the CF of the emergent line Stokes parameters, $\mathbf{C}_l$, and the Stokes line depression CF, $\mathbf{C}_R$.

$\mathbf{C}_R$ is obtained by solving the transfer equation for $\mathbf{R} = \mathbf{1} - \mathbf{I}/I_c$ (Grossmann-Doerth et al. 1988; Rees et al. 1989). According to Murphy (1990) $\mathbf{C}_R$ may be written as

$$\mathbf{C}_R = \ln(10)\,\mathbf{O}(0,\tau_c)\frac{I_c(\tau_c)}{I_c(0)}\left[1 - \frac{S_l(\tau_c)}{I_c(\tau_c)}\right]\Omega(\tau_c)\mathbf{1}. \quad (26)$$

Using Eq. (13) this can easily be rewritten to

$$\mathbf{C}_R = \frac{\mathbf{C}_l(\tau_c)}{I_c(0)}\left[\frac{I_c(\tau_c)}{S_l(\tau_c)} - 1\right]. \quad (27)$$

Although Eq. (27) is not to be recommended for determining one CF from the other (particularly $\mathbf{C}_l$ from $\mathbf{C}_R$), due to numerical instability, it does allow us to predict qualitative differences between $\mathbf{C}_R$ and $\mathbf{C}_l$.

1. The ratio between $\mathbf{C}_R$ and $\mathbf{C}_l$ is the same for all Stokes parameters.
2. For an absorption line $\mathbf{C}_R$ peaks higher in the atmosphere than $\mathbf{C}_l$. This effect is largest in the line wings, i.e. when $\mathbf{C}_l$ peaks low in the atmosphere. This property is obtained by noting that for $\tau_c \gtrsim 1, I_c \approx S_l(\tau_c) \approx B_\nu$, while at $\tau_c \ll 1$ for sufficiently strong lines $I_c \approx I_c(0) \gg S_l(\tau_c)$. It also follows therefrom that the ratio $C_{R,I}/C_{l,I}$ changes strongly across a line, being largest in the cores of strong absorption lines.
3. $\mathbf{C}_R$ has opposite signs for emission or absorption, while $\mathbf{C}_l$ has the same sign. For an absorption line with an emission core (e.g. the Mg I 12.32 μm line) $\mathbf{C}_R$ should show both signs, as can be seen by considering $(\frac{I_c}{S_l} - 1)$ as a function of height and keeping in mind that for an emission line $S_l > I_c$.

6. Numerical computations

We have incorporated the new Stokes CFs derived in Sect. 3 into the Stokes profile synthesis routine of Murphy & Rees (1990), which solves the Unno-Rachkovsky equations using the DELO technique for given line and continuum source functions, absorption coefficients, damping parameters, Doppler widths, Doppler shifts and magnetic parameters. This code, described in detail by Murphy (1990), already possesses the ability to compute $\mathbf{C}_R$ and $\mathbf{C}_t$.

The source functions and absorption coefficients for the current tests are obtained (in NLTE) from version 2.0 of MULTI (Carlsson 1986). The input atomic data to this code are the same as those used by Carlsson et al. (1992) and by Bruls & Solanki (1993a, b), the details of which are irrelevant for the aims of the present paper.

We have computed the Stokes profiles along with the 3 different Stokes CFs, $\mathbf{C}_t$, $\mathbf{C}_l$ and $\mathbf{C}_R$, of a Mg I and a number of Fe I lines. In the following we discuss a few illustrative examples chosen from a larger set of computations.

6.1. Non-magnetic contribution functions

We begin with a comparison between the 3 CFs in the absence of a magnetic field. Figure 1 shows the Stokes I, or intensity profiles (top row) of Fe I 512.77 nm, a weak line, Fe I 438.35 nm, a strong line, and Mg I 12.32 μm, an unusual line since it is composed of absorption wings and an emission core. CFs at different wavelengths are plotted below each profile: $C_{t,I}$ (dashed), $C_{R,I}$ (solid) and $C_{l,I}$ (dotted). Some points are immediately apparent from the figure.

1. $C_{t,I}$ differs significantly from the other CFs for relatively weak absorption (i.e. throughout the λ 512.77 nm line and in the wing of λ 438.35 nm in Fig. 1). There it mainly reflects the contribution to the continuum and is of little use as a diagnostic, as is well known.
2. The relative amplitude of, or integral over $C_{l,I}$ and $C_{R,I}$ changes across the line. This is particularly noticeable for λ 438.35 nm. $\int C_{R,I}\,\mathrm{d}\log\tau \sim R_I$, as expected, whereas $\int C_{l,I}\,\mathrm{d}\log\tau$ shows a more complex behavior, being strongest in the line flanks. $\int C_{t,I}\,\mathrm{d}\log\tau$ is, of course, always largest in the continuum.
   Because $\int C_{R,I}\,\mathrm{d}\tau_c \sim R_I$ it is straightforward to determine a CF, $C_{R,W}$, to the equivalent width, $W_\lambda = \int R_I\,\mathrm{d}\lambda$:
   $$C_{R,W} = \int_{-\infty}^{\infty} C_{R,I}(\lambda,\tau)\,\mathrm{d}\lambda. \quad (28)$$
   Similarly, a $C_{l,W}$ can be defined, but is less straightforward, since it must first be normalized and then weighted with $R(\lambda)$ before integration over λ. This constitutes a certain advantage for C_R.
3. The peak of $C_{t,I}$ lies either at the same τ_c or deeper in the atmosphere than the peak of $C_{l,I}$, which in turn lies deeper than the peak of $C_{R,I}$, in accordance with Eq. (27). Also in accordance with that equation, the difference, $\Delta\log\tau_c$, between the optical depth of the peaks of $C_{l,I}$ and $C_{R,I}$ is smallest when the absorption is largest, i.e. at a position at which $S_l \ll I_c$ ($\Delta\log\tau_c \approx 0.2$ in the case of λ 438.35 nm), and it is largest for weak absorption, $S_l \approx I_c$ ($\Delta\log\tau_c \approx 0.5$ in λ 512.77 nm and in the wing of λ 438.35 nm).
4. The most interesting behavior is shown by the CFs to the Mg I 12.32 μm line. Whereas $C_{t,I}$ and $C_{l,I}$ are almost identical, showing a single-peaked hump, $C_{R,I}$ is more complex, particularly near the line core. Negative $C_{R,I}$ implies emission, and the negative lobe of $C_{R,I}$ gives the contribution to the line's central emission peak, while the positive lobe contributes to the wide absorption trough. Thus $C_{R,I}$ distinguishes between the contributions to the two main features of this line, while $C_{l,I}$ and $C_{t,I}$ do not.
   From various tests, e.g. the Zeeman splitting of the 12.32 μm line in the presence of a height-independent field, we conclude that the emission peak of this line is formed near the τ_c at which $C_{R,I}$ has its negative maximum. Thus, at least for this line, $C_{R,I}$ is of far greater diagnostic value than $C_{l,I}$.

6.2. Contribution functions for magnetically split lines

In Fig. 2 we show the Stokes I and V profiles of the Landé $g = 3$ line Fe I 630.25 nm (top row), as well as the corresponding CFs at three wavelengths for a field strength $B = 0$ (left column) and $B = 3000$ G (middle and right columns). Again all three CFs ($\mathbf{C}_t$, $\mathbf{C}_R$ and $\mathbf{C}_l$) have been plotted. This plot (and others like it) confirm Eq. (27) for magnetically split lines. We also learn from the plot that $\mathbf{C}_R$ and $\mathbf{C}_l$ reflect the line profile changes produced by the magnetic field equally well, much more clearly than $\mathbf{C}_t$ (cf. Grossmann-Doerth et al. 1988). The Stokes Q and U profiles (not plotted) as well as other computations confirm the above results. The remarks made in Sect. 6.1 are seen to be valid for the magnetic case as well.

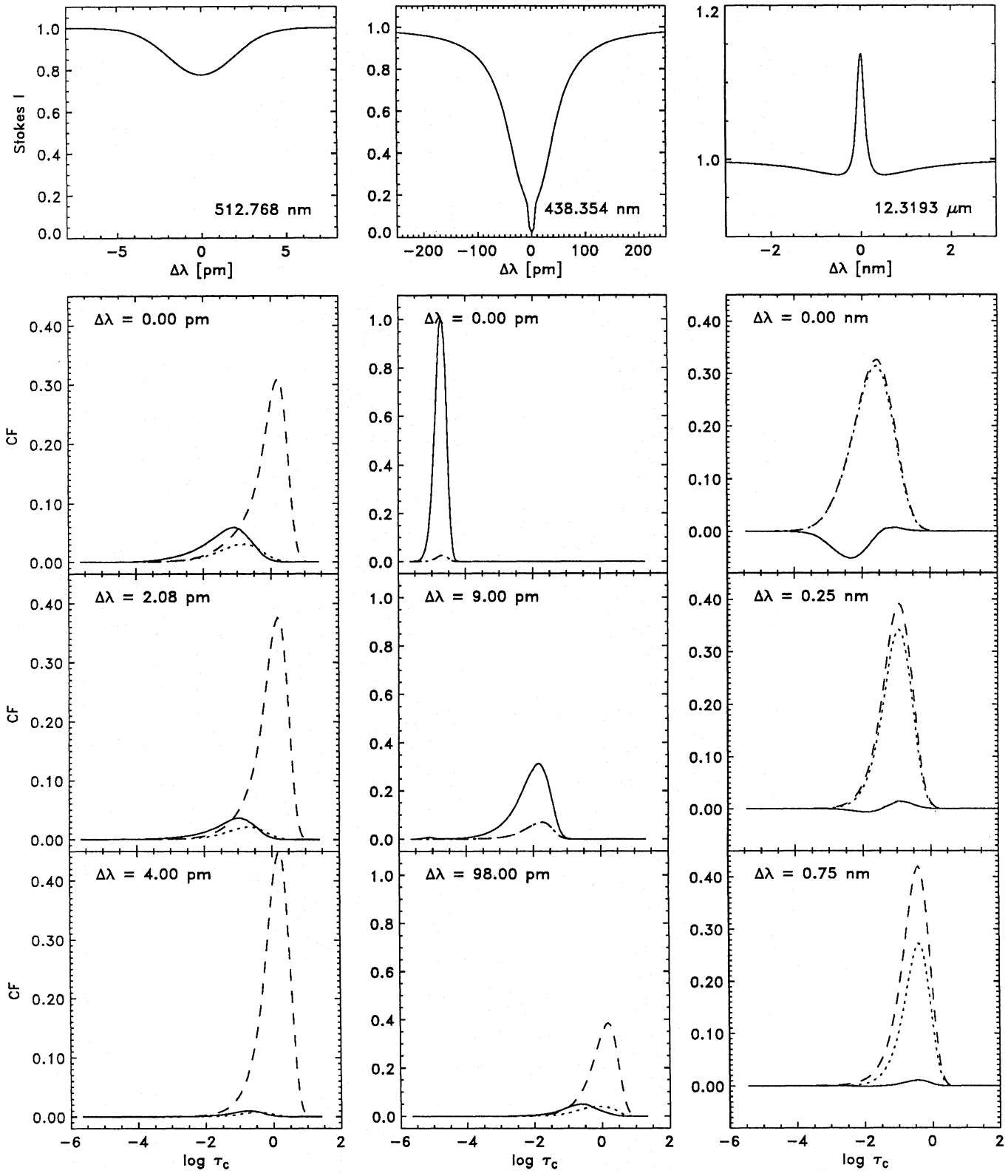

Fig. 1. *Top row:* Line profiles for Fe I 512.77 nm (weak), Fe I 438.35 nm (strong) and Mg I 12.32 μm (with emission core on absorption wings) for zero magnetic field. *Second to last row:* Comparison of corresponding contribution functions $C_{R,I}$ (solid), $C_{l,I}$ (dotted) and $C_{t,I}$ (dashed) for each line at three different wavelengths from line center indicated at the top of each panel. Note that in the second and third rows of the central column (438.354 nm) $C_{l,I}$ and $C_{t,I}$ are identical

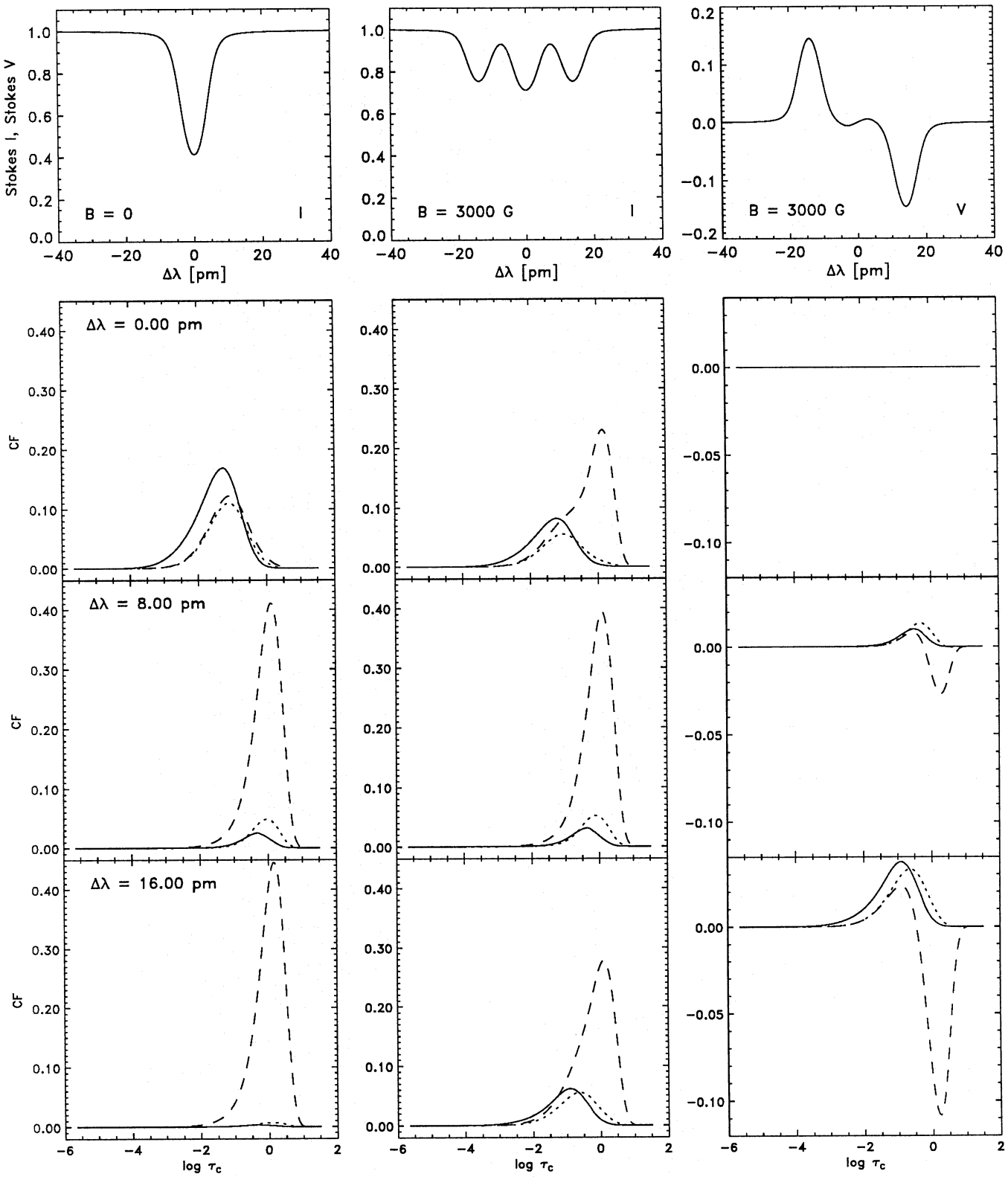

Fig. 2. *Top row:* Line profiles for Fe I 630.25 nm: Stokes I for $B = 0$ (first column) and $B = 3000$ G (second column), and Stokes V for $B = 3000$ G (third column). *Second to last row:* Comparison of corresponding contribution functions C_R (solid), C_l (dotted) and C_t (dashed) at three different wavelengths, for Stokes I (first two columns) and for Stokes V (third column)

7. Conclusions

We have extended the CF for the emergent line radiation, C_l, introduced by Achmad et al. (1991) and Gurtovenko et al. (1991), to the Stokes vector, $\mathbf{C}_l$. We have also given an explicit expression for its computation using the DELO technique for the numerical solution of the Unno-Rachkovsky equations. We have compared $\mathbf{C}_l$ both analytically and numerically with the Stokes line depression CF, $\mathbf{C}_R$. In agreement with the conclusions of Gurtovenko et al. (1991), who considered C_l and C_R among a number of possible CFs, we find that for the intensity or the Stokes parameters of Zeeman split lines there is in general little to choose between the two CFs. Their peaks usually lie within 0.2 dex in $\log \tau_c$ in the cores of medium to strong lines and $\approx$ 0.5 dex in the line wings and the cores of weak lines. For complex lines with absorption wings and emission cores, such as the 12 μm lines, however, $\mathbf{C}_R$ has a definite advantage over $\mathbf{C}_l$ as a diagnostic tool.

As pointed out by Achmad et al. (1991) the advantage of C_l over C_R lies principally in the former's simpler applicability to stellar flux spectra. In the presence of a magnetic field the flux is no longer a useful quantity and an explicit disc integration must be carried out, since the absorption coefficient and source function in Eq. (10) are not isotropic anymore. Thus, for $B \neq 0$ $\mathbf{C}_l$ loses its main advantage over $\mathbf{C}_R$ and in most cases either one of the two CFs can be used. The differences between them do add to the uncertainty in the true height of line formation, but since the separation between the τ_c of their peaks is generally much less than their half widths, this additional uncertainty is not too significant. Not only are C_R and C_l very similar from a practical point of view, but, as pointed out by Gurtovenko et al. (1991), they are equally basic in the sense that they both describe contributions to the bound-bound transitions giving rise to spectral lines, in contrast to bound-free and free-free transitions, which are responsible for the continuum (cf. Grossmann-Doerth et al. 1988).

References

Achmad L., de Jager C., Nieuwenhuijzen H., 1991, A&A 250, 445

Bruls J. H. M. J., Solanki S. K., 1993a, A&A 273, 293

Bruls J. H. M. J., Solanki S. K., 1993b, A&A submitted

Carlsson M., 1986, A Computer Program for Solving Multi-Level Non-LTE Radiative Transfer Problems in Moving or Static Atmospheres, Report No. 33, Uppsala Astronomical Observatory

Carlsson M., Rutten R. J., Shchukina N. G., 1992, A&A 253, 567

de Jager C., 1952, The hydrogen spectrum of the Sun, Thesis, Rijksuniversiteit Utrecht, Utrecht

Grossmann-Doerth U., Larsson B., Solanki S. K., 1988, A&A 204, 266

Gurtovenko E., Ratnikova V., de Jager C., 1974, Solar Phys. 37, 43

Gurtovenko E. A., Sheminova V. A., Sarychev A. P., 1991, Solar Phys. 136, 239

Landi Degl'Innocenti E., 1976, A&AS 25, 379

Landi Degl'Innocenti E., 1987, in W. Kalkofen (ed.), Numerical radiative transfer, Cambridge University Press, Cambridge, Great Britain, p. 265

Magain P., 1986, A&A 163, 135

Mein P., 1971, Solar Phys. 20, 3

Murphy G. A., 1990, The Synthesis and Inversion of Stokes Spectral Profiles, NCAR Cooperative Thesis No. 124, High Altitude Observatory, Boulder

Murphy G. A., Rees D. E., 1990, Operation of the Stokes Profile Synthesis Routine, NCAR Technical Note NCAR/TN-348+IA, High Altitude Observatory, Boulder

Pecker J. C., 1952, Ann. d'Astrophys. 14, 115

Rees D. E., 1987, in W. Kalkofen (ed.), Numerical Radiative Transfer, Cambridge University Press, Cambridge, Great Britain, p. 213

Rees D. E., Murphy G. A., Durrant C. J., 1989, ApJ 339, 1093

van Ballegooijen A. A., 1985, in M. J. Hagyard (ed.), Measurements of solar vector magnetic fields, NASA Conference Publication 2374, p. 322

This article was processed by the author using Springer-Verlag LaTeX A&A style file version 3.